Environmental Science
Water Research & Technology

CFD-accelerated bioreactor optimization: Reducing the hydrodynamic parameter space

Journal:	*Environmental Science: Water Research & Technology*
Manuscript ID	EW-PER-09-2021-000666.R1
Article Type:	Perspective

Optimization of promising water/wastewater treatment technologies requires significant resources in terms of time, labor and cost due to complex interactions between flow, microorganisms and reactions. The use of computational fluid dynamic simulations can shrink the possible parameter space, hence decreasing scale-up optimization costs.

Journal Name

ARTICLE TYPE

Cite this: DOI: 00.0000/xxxxxxxxxx

CFD-accelerated bioreactor optimization: Reducing the hydrodynamic parameter space

Yinuo Yao,*[ab] Oliver B. Fringer,[b] and Craig S. Criddle[a]

Received Date
Accepted Date

DOI: 00.0000/xxxxxxxxxx

Optimization of bioreactor design can be experimentally challenging because of the complex interactions between hydrodynamic and biological processes. A promising prototyping strategy is the use of computational fluid dynamic (CFD) simulations to identify preferred hydrodynamic parameter spaces. In this work, we describe CFD simulations of flow in anaerobic fluidized-bed reactors (FBRs), with a focus on bed expansion and particle size. The results reveal regimes of putative high mass transfer where the diffusion layer thickness is impacted by a combination of flow velocity and particle collisions. These regimes are observed when bed expansion is narrowed from 10-70% (typically recommended) to 40-60%. Similarly, prospects for short circuiting are minimized by constraining the Archimedes number Ar of fluidized particles to $Ar > 1000$ (as opposed to the common wisdom that "smaller is better"). When membranes are added to an FBR design, fluidized particles can effectively scour and clean membranes by constraining Ar to values $Ar > 7000$ (a minimum is required). We conclude that CFD can provide valuable insights into reactor design and operation, reducing the hydrodynamic parameter space that must otherwise be explored by laboratory and pilot-scale validation thus decreasing time and cost for system optimization.

1 Introduction

Sustainability is a grand challenge for the 21st century[1]. Current human civilization is largely supported by linear economies in which resources are extracted, used, and discarded at end-of-life. This has created enormous challenges, increasing the need for circular economies based upon recycling and reuse[2–5].

Microbial processes play an integral role in the removal of organic carbon and nutrients[6–8]. The prevailing technology first developed at the turn of the 20th century is activated sludge, a process that has since been modified to enable nutrient removal. Many emerging technologies cannot cross the "Valley of Death" because they treat tiny flows (in many cases, just milliliters per day) while adoption in practical applications may require treatment of tens of millions of liters per day. As biological and hydrodynamic complexity increases, the "Valley of Death" becomes

[a] Codiga Resource Recovery Center at Stanford, Department of Civil and Environmental Engineering, Stanford University, Stanford, CA, 94305, USA. Email: yaoyinuo@stanford.edu
[b] The Bob and Norma Street Environmental Fluid Mechanics Laboratory, Department of Civil and Environmental Engineering, Stanford University, Stanford, CA, 94305, USA.

deeper. An example would be bioelectrochemical processes, such as microbial fuel cells[9] and microbial batteries[10,11], technologies that have been demonstrated at bench- and, in some cases, pilot-scale but not full-scale. Academia is a likely source for such potentially disruptive innovation but lacks access to the facilities and funding needed for long-term testing at a meaningful scale. To date, microbially-based technologies have largely relied upon experiments for optimization, but such testing is slow and costly. Not surprisingly, practitioners and utilities tend to innovate incrementally using existing systems. There is thus a great risk of locking-out innovation. A pathway for lower cost and more rapid scale-up of promising technology is needed.

In general, bioreactors can be classified as either dispersed growth systems, where substrate gradients are minimal, or attached-growth/floc-based systems, where appreciable substrate gradients drive diffusion of substrate into floc or attached biofilms as products diffuse out. The classic dispersed-growth example is activated sludge (AS), a technology that efficiently removes organic carbon in wastewater by converting soluble organics into CO_2. Active microbial biomass is concentrated by settling or membrane separation. These microorganisms are typically present as discrete cells or as floc within a size range of 2-20 μm[12,13]. This size range confers two benefits: (1) the absence of a significant diffusion layer eliminates mass transfer limitations, and (2) small particles follow flow trajectories with negligible disruption of the overall hydrodynamics. The combined effect of these processes is to weaken the dependence of biological activity on diffusion within floc or particles under well-mixed conditions, with minimal energy consumption and minimal short-circuiting. To achieve excellent mixing, vigorous bubbling is used for aeration and/or mechanical mixing. To date, most research has focused on optimization of process-related parameters such as HRT, solid retention time (SRT), and on microbial kinetic parameters with minimal hydrodynamic impacts. By excluding hydrodynamics in such models, reactor design and operation are greatly simplified. Examples include, but are not limited to, prediction of biological activity using ordinary differential equations rather than partial differential equations. In contrast to dispersed growth reactions, attached growth and biofilm reactors are much more complex and more affected by process hydrodynamics. Examples would include trickling filters, granular reactors, fluidized-bed reactors, membrane-aerated reactors, microbial fuel cells, and microbial batteries. For these examples, well-mixed conditions do not insure a reduction in the hydrodynamic parameter space. The parameter space in complex systems (such as microbial flocs, biofilm-coated particles and biofilm-coated porous materials, and electrically conductive sponge) is much larger than in dispersed-growth reactors, and a thicker diffusion layer can increase mass transfer limitations. In addition, floc and BC-Ps do not necessarily follow the flow and flow-particle interactions can eventually alter the flow trajectories, creating more complex hydrodynamics. As a result, biological activity and overall treatment efficiency depend upon local hydrodynamics. To optimize reactor design and operation, a quantitative understanding of hydrodynamic-related parameters such as particle Reynolds number, porosity and Archimedes number is critical. By including hydrodynamic-related parameters, the total number of parameters (both hydrodynamic- and process-related) increases, resulting in drastic increases in resources in terms of cost and time and the number of experiments required for optimization. Simultaneously, the likelihood of obtaining optimal performance diminishes due to the high dimensional parameter space.

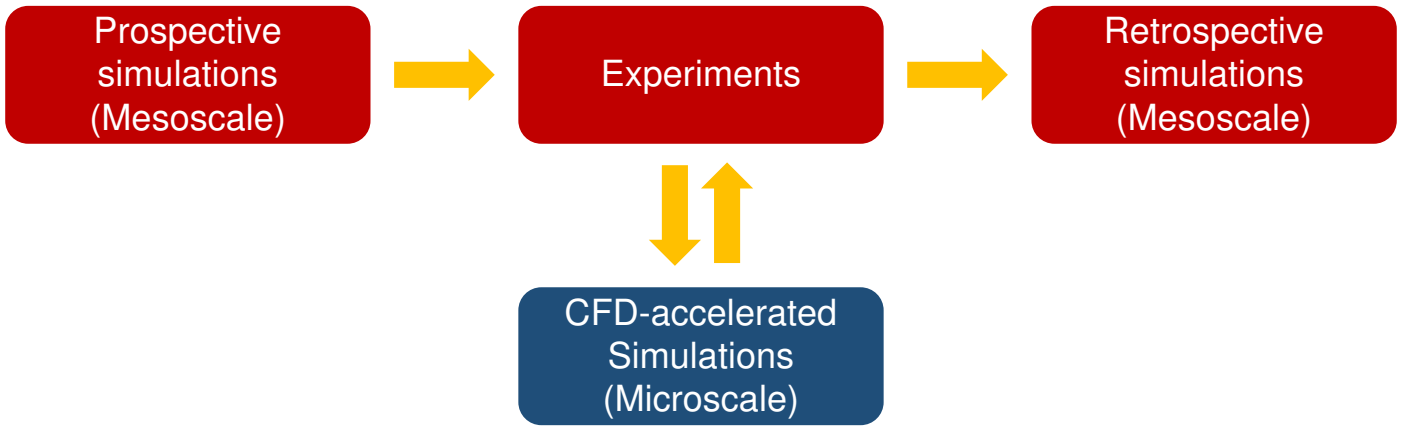

Fig. 1 Workflow of CFD-accelerated scale-up. The red boxes indicate conventional CFD applications for reactor optimization. The blue box highlights iterative and integrative simulation and experiments. Mesoscale refers to simulations where the size of the computational domain is on the order of meters and the shape resembles an industrial reactor. Microscale refers to simulations at scales much smaller than reactors, on the order of millimeters or even microns.

2 Computational fluid dynamics

Computational fluid dynamics (CFD) uses numerical methods to study problems that involve fluid flows. Over the past few decades, advances in computational power and methods have expanded the range of problems that can be addressed using CFD. A review by Karpinska and Bridgeman[14] has evaluated different strategies and models for optimization of wastewater treatment. In wastewater treatment (Figure 1), CFD can (1) prospectively preview macroscopic reactor hydrodynamics and (2) retrospectively improve current design and operation. Studies are carried out sequentially by first comparing simulations with experimental results (i.e., historical results from an existing system in retrospective applications or from a similar system in prospective applications) then conducting simulations by varying a parameter of interest. These studies are mostly conducted at the mesoscale where the size of the computational domain is on the order of meters and the shape resembles an industrial reactor. The main disadvantage of this approach is loss of microscale information where microscale refers to simulations investigating scales that are much smaller than reactors and in the order of micron or millimeters (i.e, interactions between small particles on an industrial fluidized-bed reactor). As such, most research adopting this approach focuses on macroscopic properties such as flow short-circuiting, reactor mixing and oxygen transfer efficiency using commercial software[15–17]. For dispersed growth reactors, with a reduced hydrodynamic parameter space, CFD studies have focused on aeration and mixing. Another useful CFD application is disinfection. In this case, short-circuiting is minimized to enable efficient pathogen removal, a goal that must be balanced against the need for minimization of disinfection byproducts[18–20]. In these applications, the simulations are reactor-specific, so the knowledge gained from one system does not necessarily translate to another.

In more complex reactors (attached-growth or floc-based), the parameter space increases significantly due to local interactions between hydrodynamics and biological activity. Aerobic fluidized bed reactors require aeration and mixing simulations, but also guidelines on bed expansion, particle size, and other carrier properties of

interest. Focusing on aeration and mixing alone is unlikely to result in optimized design and performance. In addition, because most interactions occur at the microscale, ignoring microscale properties (e.g., floc diffusion layer or floc-floc interactions) with a singular focus on macroscopic properties (bed expansion or mixing) is also unlikely to lead to correct conclusions. Understanding of systems that have shared physics can expedite translation across systems. Resources spent on understanding of one system would benefit other similar systems. An example is the effect of Archimedes number (a combination of particle and fluid properties) in upward flow reactors. A quantitative understanding of this number would be beneficial to both non-fluidized granular reactors and fluidized-bed reactors. The focus of this approach is not to identify the exact values for optimized parameters but rather to reduce the parameter space within which optimized parameters fall. By narrowing this space, reactor-specific experimental studies can be more targeted, enabling more efficient optimization and scale-up with fewer resources.

In this paper, we propose a new framework for bioreactor optimization: a computational strategy in which CFD is used to understand fundamental interactions involving fluid flow, particles, microorganisms, membranes, and other porous materials. We envision that this approach will enable deeper insight into the underlying physics and accelerated optimization. We use the Staged Anaerobic Fluidized-bed Membrane bioreactors (SAF-MBR) as a case study to demonstrate the feasibility and potential of this framework.

3 A case study: Staged Anaerobic Fluidized-bed Membrane Bioreactors

The SAF-MBR is a recently developed biocarrier-based anaerobic treatment technology[21,22]. Aeration is eliminated because the active microorganisms are obligate anaerobes that do not tolerate oxygen. Energy is recovered as methane, enabling net energy-positive secondary treatment of domestic wastewater[23]. Because they are slow-growing, the anaerobes also generate fewer biosolids for disposal. These properties make the SAF-MBR more attractive than conventional aerobic processes, such as AS[24].

The SAF-MBR consists of two reactors in series with a conventional anaerobic fluidized-bed reactor (AFBR) followed by an anaerobic membrane bioreactor (AnMBR). AFBRs have been widely used to treat industrial wastewater where the Chemical Oxygen Demand (COD) and Biochemical Oxygen Demand (BOD) are much greater than domestic wastewater. In SAF-MBR 1.0, the AFBR discharges to a particle-sparged membrane bioreactor (P-MBR), in which fluidized granular activated carbon (GAC) functions as both a biocarrier of slow-growing microorganisms (inside the GAC pores) and as a scouring agent for cleansing of membranes and prevention of biofouling[21,22,24,25]. This strategy successfully controlled membrane biofouling in a pilot-scale SAF-MBR[21,26], but also led to particle abrasion and damage of the polymeric membranes[27]. As noted by Shin et al.[27], the GAC used in the P-MBR contained two size fractions - one at 1.18 - 1.4mm (29%) and a second at 1.70 -4.00mm (47%). Significant membrane damage occurred in the lower region of the membranes, and this damage was attributed to the larger GAC fraction. In subsequent pilot-scale tests of SAF-MBR 2.0[23], membrane sparging was accomplished with biogas bubbles rather than solid particles.

The hydrodynamics of fluidized-bed reactors have been investigated experimentally[28,29] and with simulations[30–34], but membrane bioreactor studies of microbial activity have largely focused on experimental testing[35,36].These studies do not track particle dynamics at high volume fraction (low porosity), but instead focus on macroscopic behavior such as fluidization stability and expan-

sion[37,38]. The range of bed expansion in fluidized beds fluctuates between 20% and 70% with a qualitative understanding that low expansion leads to flow short-circuiting and high expansion leads to biofilm loss. The optimal bed expansion or porosity is thus an open question. At present, most studies focus on bed expansion without considering the impacts of particle properties such as Archimedes Ar (or Galilei Ga) number on the optimal bed expansion where Ar is defined as

$$Ar = Ga^2 = \frac{(s-1)gd_p^3}{\nu^2}, \quad (1)$$

where $s = \rho_p/\rho_f$ is particle-fluid density ratio, d_p is the clean particle diameter, g is the gravitational acceleration and ν is the kinematic viscosity of water. Qualitatively, small particles are preferred to enable more efficient mass transfer and enhanced biological activity. Aslam et al.[26] studied the effects of three different particles (PET beads, silica and GAC) on membrane scouring efficiency and concluded that PET beads are best.

3.1 Upflow velocity and porosity

In fluidized-bed reactors, upflow velocity controls bed expansion and hence porosity. Understanding particle dynamics as a function of porosity gives important insights into the biological activity and design and operation of reactors. Recently, Yao et al.[32] investigated particle dynamics by varying upflow velocity in simulations of a monodispersed/single-size fluidized bed with particle properties similar to those of pilot-scale and lab-scale reactors[21]. Within FBRs, porosity controls both the horizontal mixing and collisions between particles. Since no horizontal flow is generated at the inlet, horizontal mixing is mainly due to momentum transfer from the vertical to horizontal directions due to particle fluctuations. At low porosity, most fluctuations are induced by weak collisions. At intermediate porosity, collisions and hydrodynamic effects become equally important, leading to an increase in particle velocity fluctuations and stronger collisions. At high porosity, hydrodynamic effects dominate, and collisions are diminished.

3.1.1 Hypothetical impacts on biofilm detachment

Accurate quantification of biofilm detachment rate provides valuable information in modeling biofilm reactor dynamics, such as the height of expanded beds and insight into reaction- and mass-transfer limitations[39]. The overall biofilm detachment rate b_t is modeled as a combination of first-order cell decay and mechanical detachment:

$$b_t = b + b_{det}, \quad (2)$$

where b is the first-order cell decay constant and b_{det} is the mechanical detachment rate. Typically, $b << b_{det}$ for most the engineered applications such that $b_t \approx b_{det}$. There are two types of detachment (continuous and discrete) and three mechanisms (shear stress, abrasion, and sloughing). The shear stress is due to flow, while abrasion is due to collisions between particles. Since sloughing is typically described as a discrete probabilistic event that might lead to breakup of the entire biofilm[40], most models do not consider it. Chang et al.[41] modeled b_{det} as

$$b_{det} = -3.14 + 0.0335C_p + 19.3Re_{p,b} - 3.46\sigma, \quad (3)$$

where C_p is the particle concentration in the fluidized bed, $Re_{p,b} = u_0 d_b/\nu$ is the biofilm-covered particle Reynolds number, u_0 is the upflow velocity in the fluidized bed, d_b is the diameter of the BC-P and σ is the shear stress. The author assumed that C_p, $Re_{p,b}$ and σ account for abrasion, turbulence and shear stress, respectively. The main challenge with this model is related to decoupling flow ($Re_{p,b}$) and abrasion effects (C_p)

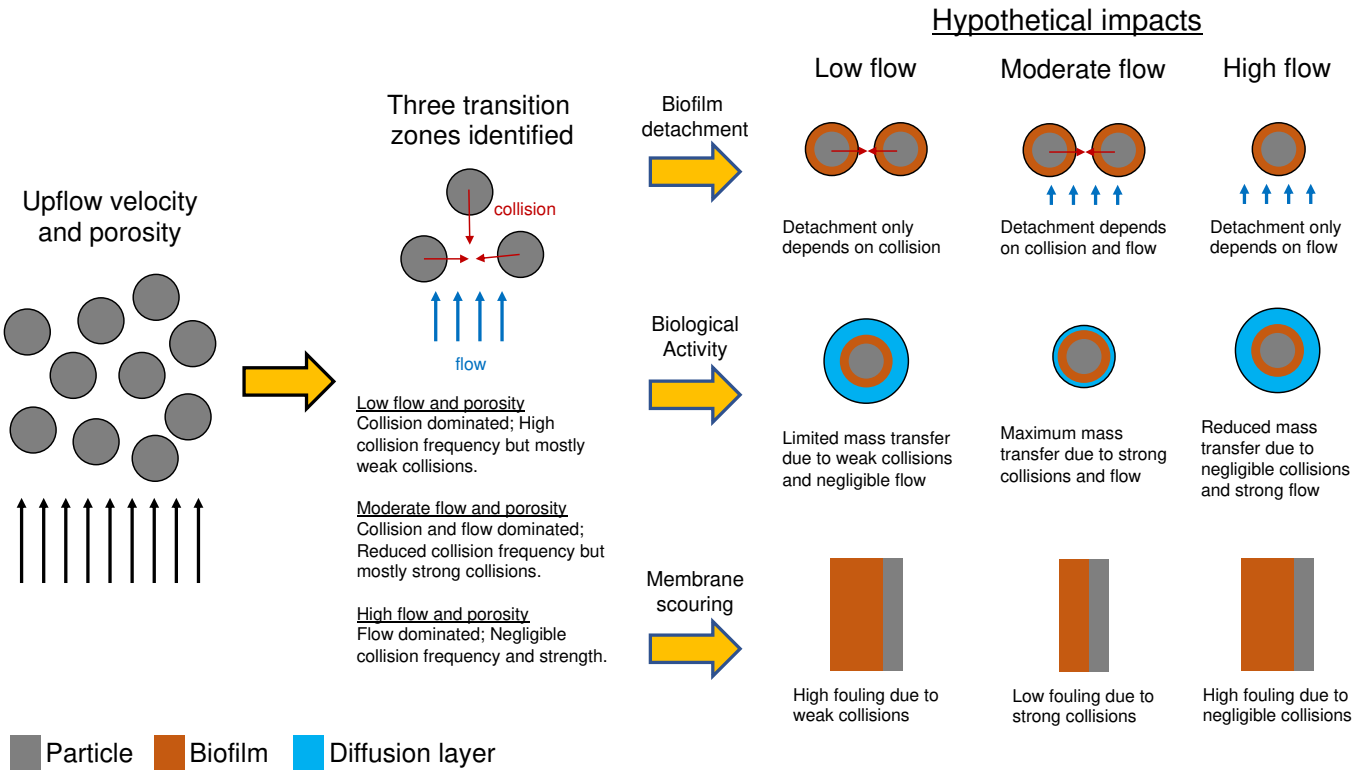

Fig. 2 Hypothetical impacts of upflow velocity and porosity on fluidized-bed reactor modeling, design and operation.

where both C_p and $Re_{p,b}$ are functions of porosity.

Nicolella et al.[42] constructed an empirical model for a fluidized-bed reactor based on dimensional analysis and showed that the normalized detachment rate $\widehat{b} = d_p \widetilde{b}_{det}/\rho_f \nu$ is given by

$$\widehat{b} = 1.95 \times 10^{-10} Re_{p,c}^{1.49} d_*^{2.67}, \quad (4)$$

where $\widetilde{b}_{det}$ is the amount of biofilm detached per unit area and time, $Re_{p,c} = d_p u_0/\nu$ is the clean particle Reynolds number and $d_* = d_b/d_p$ is the diameter ratio of a biofilm-covered to a clean particle. An interpretation of this model is that $Re_{p,c}$ represents the effects of clean particle-related flow whereas d_* includes the effects of biofilm thickness on the detachment rate. The effect of flow includes both turbulence and abrasion as compared to equation 3[41]. Interestingly, detachment rates that were orders of magnitude higher were observed for $d_* = 3$ and $Re_{p,c} = 2.3 - 2.7$ which cannot be explained by this model, although one plausible explanation is that detachment occurs near the inlet where turbulence is strongest. Overall, this model better parameterizes the mechanical biofilm detachment rate in the sense that there is much less cross-correlation between parameters. Instead of considering both flow and abrasion, Gjaltema et al.[43] assume that abrasion is the only dominant detachment mechanism in an airlift reactor and used a model to estimate the energy of abrasion.

All of the above models are unable to decouple flow and abrasion or are limited to abrasion. By comparing high- and low-strength FBRs, Shin et al.[44] successfully modeled low-strength FBRs by assuming small b_{det}. By examining particle dynamics in a fluidized bed, Yao et al.[32] discovered that collisions dominate over hydrodynamic effects at low porosity. At intermediate porosity, both collisions and hydrodynamic effects are important while hydrodynamic effects dominate at

higher porosity. The combination of effects of wastewater strength and hydrodynamics implies that the biofilm detachment rate in a fluidized-bed reactor can be modeled with a stepwise function

$$b_{det} = \begin{cases} b_{col} f(C_{COD}), & \text{for } \varepsilon < \varepsilon_{c1}, \\ (b_{col} + b_{hydro}) f(C_{COD}), & \text{for } \varepsilon_{c1} \leq \varepsilon < \varepsilon_{c2}, \\ (b_{hydro}) f(C_{COD}), & \text{for } \varepsilon \geq \varepsilon_{c2}, \end{cases} \quad (5)$$

where $f(C_{COD})$ is a function that relates b_{det} and chemical oxygen demand (COD) concentration of wastewater, ε is the porosity, ε_{c1} and ε_{c2} are critical porosities representing the boundaries of the different regimes, and b_{col} and b_{hydro} are the detachment rates associated with collisional and hydrodynamic effects. Biofilm detachment is likely maximized to the coexistence of two different mechanisms at intermediate Reynolds numbers. Although further experimental validation is required, observing how particle dynamics change in fluidized bed simulations provides insight into biofilm detachment and how detachment rates might best be modeled. Furthermore, because ε_{c1} and ε_{c2} vary with particle properties such as diameter and density, a universal scaling law can be developed that confirms and generalizes this approach for different particle diameters and densities.

3.1.2 Hypothetical impacts on mass transfer and biological activities

Fluidized-bed reactors are known for their excellent mass transfer rate. When applied for wastewater treatment, the AFBR can either be mass transfer limited or reaction rate limited. The latter usually occurs in shallow and fully-penetrated biofilms where substrates are metabolized at a much slower rate than diffusion enables. Buffiere et al.[35] discovered that the methanogenic step requires deep biofilms while acidogenesis only requires shallow biofilms for treatment of high-strength wastewater. Conflicting results have been reported where increases in flow rate can either increase[45] or decrease[46] the mass transfer rate. Nicolella et al.[47,48] discovered that mass transfer of biofilm-covered particles in airlift reactors is roughly 15% lower than that of clean particles.

Due to the serial nature of process kinetics, with mass transfer preceding biochemical kinetics, overall reactions can be mass transfer-limited when the reaction step is fast or they can be reaction-limited when the mass transfer step is slow[35]. In AFBRs, the particle Reynolds number based on superficial velocity leads to collisions and hydrodynamic effects that control mass transfer. Higher flow rates reduce the thickness of the diffusion layer thereby enhancing mass transfer. Similarly, more frequent collisions disrupt the diffusion layer reducing its thickness in fluidized-bed electrochemical cells[49]. The effect of collisions alone can be accurately described by the collision pressure which is known to have a maximum and zeros for both single-particle ($\varepsilon \approx 1$) and close-packed reactors ($\varepsilon \approx 0.4$)[43,50]. After close examination of particle dynamics in fluidized bed simulations, Yao et al.[32] suggested that mass transfer is most likely maximized within the intermediate porosity regime at which point collisions and hydrodynamic factors are equally important, leading to optimal biological performance. Although not yet experimentally validated, pilot- and lab-scale reactors operated at this intermediate porosity (bed expansion of 40% to 60%) have achieved optimal treatment performance[21,23,51].

3.1.3 Hypothetical impacts on membrane fouling control

The primary role of the P-MBR is to retain particulate biodegradable organic matter in the reactor because more time is required for hydrolysis. The main challenge is to prevent membrane

biofouling, which can be accomplished by either particle- or gas-sparging. Particle-sparged operation enables low energy demand[52] but can lead to severe membrane damage in the lower region of the reactor[53]. Moreover, due to non-uniform particle sizes, the fluidized bed in the P-MBR forms segregated layers of particles with larger particles (2-4 mm) located at the bottom of the bed. Yao et al.[32] found that the maximum collision frequency is attained at intermediate porosity for 2 mm particles. Low porosity is characterized by more frequent weak collisions while high porosity is dominated by flow rather than collisions. Comparing the collision frequency as a function of porosity by Yao et al.[32] and the membrane integrity study by Shin et al.[27] with similar particle sizes, the porosity of the lower region in the pilot-scale P-MBR corresponds to the region of maximum effective collisions from the simulations. This result implies that membrane scouring efficiency can be controlled by varying porosity, therefore the bed expansion. Maximum membrane scouring is attained at the porosity with maximum collisions. To avoid membrane damage, varying the porosity to deviate from the maxima say, by reducing or increasing it, is likely to eliminate membrane damage. As discussed below, instead of switching to alternative membrane fouling control methods, studying the effects of the Archimedes number enables a retrospective modification to both new and existing reactors.

3.2 Particle properties and the Archimedes number

In addition to operating parameters such as upflow velocity and porosity, choosing optimal or appropriate design parameters (i.e. Archimedes number) is critical. As discussed in the previous section, particles with low Archimedes number are preferred for better mass transfer in the AFBR. In reality, particles with the same properties are usually used for the P-MBR. Aslam et al.[26] attempted to relate particle properties such as materials, diameter and density to membrane scouring efficiency and concluded that larger particles are better at membrane fouling control. Recently, Yao et al.[33] elucidated the role of the Archimedes number on particle dynamics in a fluidized bed. The Archimedes number combines different particle properties into a single dimensionless number. Based on the simulations, the normalized particle velocity fluctuation decreases as the Archimedes number increases, indicating that the particles experience weaker effects of wake interactions in which the particle is weakly affected by neighbouring particles. By using Voronoï tessellation, particle clustering is identified and the results suggest that Archimedes number has a strong inverse relationship on particle clustering lifespan such that an increase in Archimedes number strongly decreases the lifespan. Therefore, applications with low Archimedes number are characterized by long-lived clusters while applications with high Archimedes number are characterized by short-lived clusters. The mechanism governing the lifespan of particle clusters is the collision frequency. Increasing the Archimedes number increases the collision frequency, creating conditions more favorable for cluster breakup, leading to short-lived clusters.

3.2.1 Hypothetical impacts on flow short-circuting

A common practice in the operation of fluidized-bed reactors in wastewater treatment is to use small particles that enhance both mass transfer and surface contact. In analogy to boundary layer thickness, the diffusion layer thickness scales as

$$L \sim \sqrt{\frac{D d_p}{\tilde{u}}}, \tag{6}$$

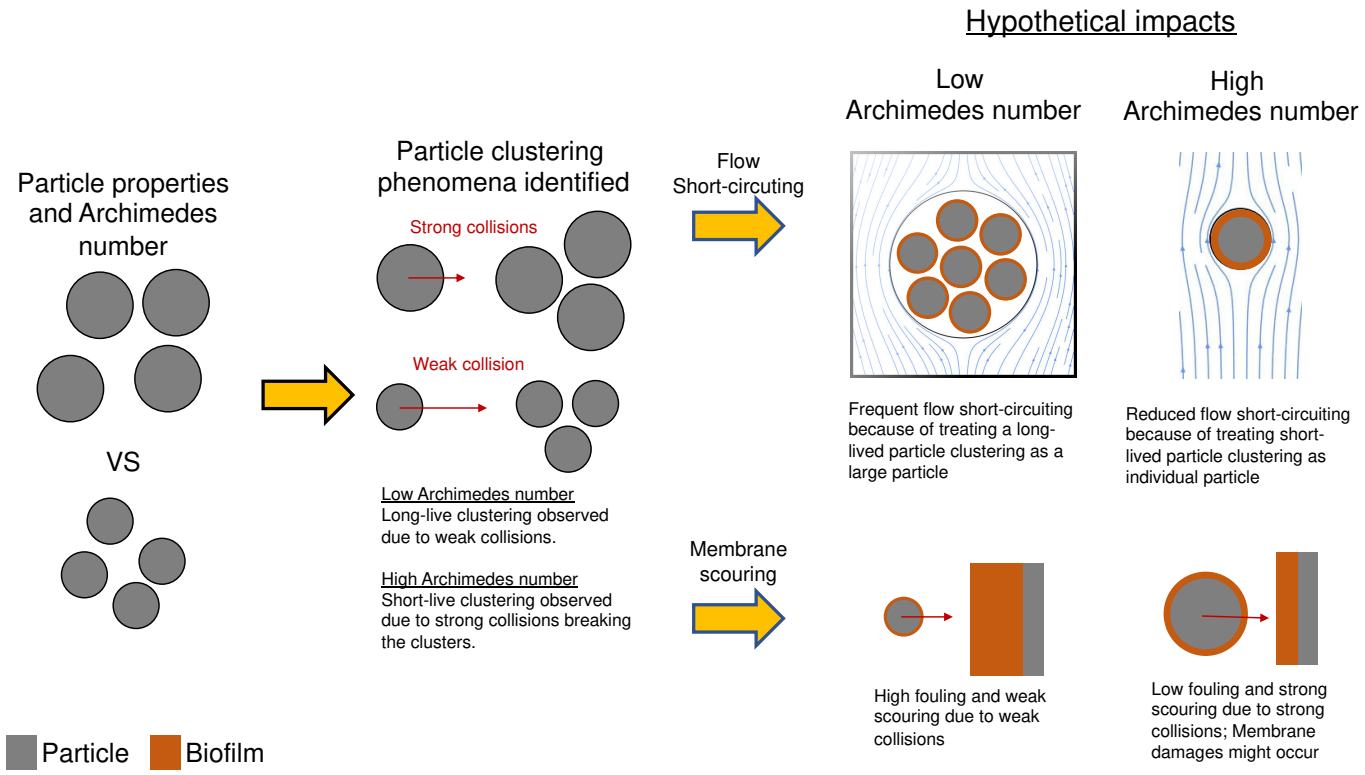

Fig. 3 Hypothetical impacts of particle properties and Archimedes number on fluidized-bed reactor modeling, design and operation.

where D is the diffusion coefficient of the targeted compound and $\tilde{u}$ is the fluid velocity over the particle. From equation 6, L decreases as d_p decreases and $\tilde{u}$ increases. Therefore, smaller particles are less likely to be mass-transfer limited due to the reduced diffusion layer thickness. In practice, particle size is chosen based on the minimum particle size or Archimedes number that can be easily retained in the system. However, contrary to popular opinion, Yao et al.[33] found that particles with $Ar < 1000$ tend to form prolonged clusters while particles with $Ar \geq 1000$ are more likely to form short-lived clusters. Long-lived clusters tend to behave like a single large particle, resulting in more fluctuations in particle dynamics. This result suggests that flow short-circuiting is more likely to occur when fluid flows over a large particle cluster rather than each individual particle, resulting in reduced surface contact and exchange between biofilm and bulk fluid.

3.2.2 Hypothetical impacts on scouring frequency and membrane lifetime

Besides porosity, particle properties controlling the Archimedes number can affect membrane scouring efficiency. As demonstrated in many papers[26,50,54], larger particles (high Archimedes number) tend to result in more frequent impact collisions that ultimately damage the membrane over time while small particles (low Archimedes number) do not induce effective collisions and hence minimal membrane scouring[33]. Therefore, choosing particles with appropriate Archimedes number is critical. To ensure effective membrane biofouling control, particles with $Ar > 1000$ are likely to have effective collisions[33]. Therefore, the minimum Archimedes number for effective membrane scouring is $Ar \approx 1000$. For better scouring efficiency, particles with higher

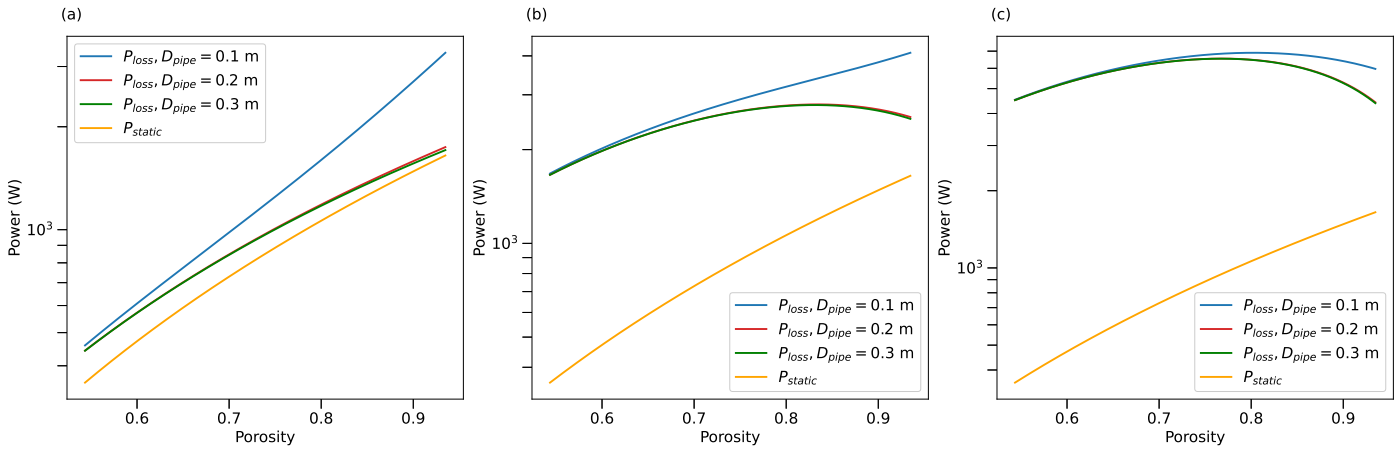

Fig. 4 Power requirement as a function of porosity for (a) $Ar = 2.3 \times 10^4$, (b) $Ar = 1.2 \times 10^5$ and (c) $Ar = 2.3 \times 10^5$.

Archimedes number will be more effective when there is a risk of membrane damage.

To alleviate membrane damage due to particle scouring, both the frequency and energy impacts of collisions must be reduced. This can be achieved by operating the P-MBR at a porosity that favors weaker collisions. Collision frequency and strength can both be reduced by changing porosity (both by increasing and decreasing it). Because the expanded fluidized particles must be able to access to the entire membrane module in order to provide effective scouring, and because the fluidized-bed height is predetermined, the total mass of particles must change if the upflow velocity changes. The disadvantage of adding more particles (reducing porosity) is that this leads to higher headloss and increased pumping costs. To increase porosity, a higher flow rate, hence a higher power requirement, is essential. Since the total headloss is proportional to both the hydrostatic pressure loss and pipe friction loss, a more detailed analysis of power requirements is required to determine the optimal flow rate. As an example, figure 4 shows the power requirement as a function of porosity for different Archimedes numbers Ar (model details can be found in the Supplementary Information). As shown, when the recirculation pipe diameter $D_{pipe} > 0.2$ m, D_{pipe} is no longer an important parameter. For low Ar, the power requirement is dominated by the static head loss, and the wastewater must be pumped from the bottom to the top of the reactor, leading to a monotonically increasing function of Ar. For high Ar, the power needed to fluidize the particles exceeds static headloss, leading to a parabolic function of Ar. Therefore, to reduce high energy collisions, the flow rate must be reduced for small Ar and can be increased or decreased for high Ar depending on the power requirements.

4 Conclusion and outlook

Simulations of particle dynamics in fluidized-bed reactors using CFD suggest that the parameter space for optimal bed expansion should decrease from 10%-70% to 40%-60% because optimal mass transfer is more likely to occur when both collisional and hydrodynamic forces are comparably important. To design an efficient fluidized-bed reactor, particles with $Ar > 1000$ should be chosen to avoid flow short-circuiting due to particle clustering. Similarly, particles with $Ar > 1000$ or preferably $Ar > 7000$ are needed to induce appreciable membrane scouring. The impact of membrane scouring can be adjusted by varying the porosity or flow rate.

Overall, high-fidelity CFD simulations enable a

close examination of fundamental hydrodynamics within bioreactors. Although optimal design and operating conditions cannot be precisely identified, the range of parameter space requiring experimental testing can be significantly reduced, and the likelihood that optimal conditions will be identified is greater. CFD simulations provide an added tool for study of problems that are difficult to investigate experimentally. Experiments can both validate and build upon CFD results to optimize reactor performance.

Although CFD-accelerated strategies have tremendous potential for acceleration and optimization of wastewater treatment systems, more work is clearly needed. More sophisticated computational methods are needed that incorporate biological reactions. However, the main challenge in integrating biological reactions is the difference in timescales. For biological reactions, the timescales are typically much longer than the time to reach hydrodynamic steady-state. As a result, the total computational cost increases significantly, and new methods are needed to address this challenge.

Funding Sources

This work was funded by the California Energy Commission (CEC) under CEC project number EPC-16-017, the U.S. NSF Engineering Center for Reinventing of the Nation's Urban Water Infrastructure (ReNUWIt) under Award No. 1028968, and Office of Naval Research Grant N00014-16-1-2256. This paper was prepared as a result of work sponsored in part by the California Energy Commission. It does not necessarily represent the views of the Energy Commission, its employees, or the State of California. Neither the Commission, the State of California, nor the Commission's employees, contractors, or subcontractors makes any warranty, express or implied, or assumes any legal liability for the information in this paper; nor does any party represent that the use of this information will not infringe upon privately owned rights. This paper has not been approved or disapproved by the Commission, nor has the Commission passed upon the accuracy of the information in this paper.

Conflicts of interest

There are no conflicts to declare.

Notes and references

1 T. Dooley, *Thirsting for a Future: Water and Children in a Changing Climate*, United Nations Children's Fund, The (UNICEF), 2017.

2 M. Smol, C. Adam and M. Preisner, *J. Mater. Cycles Waste Manage.*, 2020, **22**, 682–697.

3 P. H. Nielsen, *Microb. Biotechnol.*, 2017, **10**, 1102–1105.

4 E. Neczaj and A. Grosser, *Proc. AMIA Annu. Fall Symp.*, 2018, **2**, 614.

5 Y. D. Scherson, S.-G. Woo and C. S. Criddle, *Environ. Sci. Technol.*, 2014, **48**, 5612–5619.

6 Y. Yao, Z. Wang and C. S. Criddle, *Environ. Sci. Technol.*, 2021, **55**, 2016–2026.

7 Z. Wang, S.-G. Woo, Y. Yao, H.-H. Cheng, Y.-J. Wu and C. S. Criddle, *Water Res.*, 2020, **173**, 115575.

8 Z. Wang, Y. Yao, N. Steiner, H.-H. Cheng, Y.-J. Wu, S.-G. Woo and C. S. Criddle, *Environ. Sci.: Water Res. Technol.*, 2020, **6**, 3451–3459.

9 B. H. Kim, I. S. Chang and G. M. Gadd, *Appl. Microbiol. Biotechnol.*, 2007, **76**, 485–494.

10 X. Xie, C. Criddle and Y. Cui, *Energy Environ. Sci.*, 2015, **8**, 3418–3441.

11 X. Xie, M. Ye, C. Liu, P.-C. Hsu, C. S. Criddle and Y. Cui, *Energy Environ. Sci.*, 2015, **8**, 546–551.

12 D. Li and J. Ganczarczyk, *Research Journal of the Water Pollution Control Federation*, 1991, **63**, 806–814.

13 B.-M. Wilén and P. Balmér, *Water Res.*, 1999, **33**, 391–400.

14 A. M. Karpinska and J. Bridgeman, *Water Res.*, 2016, **88**, 861–879.

15 M. W. D. Brannock, Y. Wang and G. Leslie, *J. Memb. Sci.*, 2010, **350**, 101–108.

16 Y. Le Moullec, C. Gentric, O. Potier and J. P. Leclerc, *Chem. Eng. Sci.*, 2010, **65**, 343–350.

17 M. Gresch, M. Armbruster, D. Braun and W. Gujer, *Water Res.*, 2011, **45**, 810–818.

18 J. Ducoste, K. Carlson and W. Bellamy, *Journal of Water Supply: Research and Technology—AQUA*, 2001, **50**, 245–261.

19 D. J. Greene, B. Farouk and C. N. Haas, *J. Am. Water Works Assoc.*, 2004, **96**, 138–150.

20 J. M. Wilson and S. K. Venayagamoorthy, *Environ. Sci. Technol.*, 2010, **44**, 9377–9382.

21 C. Shin, P. L. McCarty, J. Kim and J. Bae, *Bioresour. Technol.*, 2014, **159**, 95–103.

22 J. Kim, K. Kim, H. Ye, E. Lee, C. Shin, P. L. McCarty and J. Bae, *Environ. Sci. Technol.*, 2011, **45**, 576–581.

23 C. Shin, S. H. Tilmans, F. Chen, P. L. McCarty and C. S. Criddle, *Water Res.*, 2021, **204**, 117598.

24 P. L. McCarty, J. Kim, C. Shin, P.-H. Lee and J. Bae, *Anaerobic Biotechnology*, IMPERIAL COLLEGE PRESS, 2015, pp. 211–242.

25 J. Bae, C. Shin, E. Lee, J. Kim and P. L. McCarty, *Bioresour. Technol.*, 2014, **165**, 75–80.

26 M. Aslam, P. L. McCarty, J. Bae and J. Kim, *Sep. Purif. Technol.*, 2014, **132**, 10–15.

27 C. Shin, K. Kim, P. L. McCarty, J. Kim and J. Bae, *Sep. Purif. Technol.*, 2016, **162**, 101–105.

28 R. de Felice, *Chem. Eng. Sci.*, 1993, **48**, 881–888.

29 C. Nicolella, S. Chiarle, R. Di Felice and M. Rovatti, *Water Sci. Technol.*, 1997, **36**, 229–235.

30 A. Esteghamatian, A. Hammouti, M. Lance and A. Wachs, *Phys. Fluids*, 2017, **29**, 033302–1–033302–14.

31 D. P. Willen and A. Prosperetti, *Phys. Rev. Fluids*, 2019, **4**, 014304.

32 Y. Yao, C. S. Criddle and O. B. Fringer, *J. Fluid Mech.*, 2021, **927**, A28.

33 Y. Yao, C. S. Criddle and O. B. Fringer, *J. Fluid Mech.*, 2021, **920**, A40.

34 Y. Yao, C. S. Criddle and O. B. Fringer, *Phys. Rev. Fluids*, 2021, **6**, 084306.

35 P. Buffière, J. P. Steyer, C. Fonade and R. Moletta, *Biotechnol. Bioeng.*, 1995, **48**, 725–736.

36 R. Lee, P. L. McCarty, J. Bae and J. Kim, *J. Chem. Technol. Biotechnol.*, 2015, **90**, 391–397.

37 S. Sundaresan, *Annu. Rev. Fluid Mech.*, 2003, **35**, 63–88.

38 J. F. Richardson and M. A. da S. Jerónimo, *Chem. Eng. Sci.*, 1979, **34**, 1419–1422.

39 B. E. Rittmann and P. L. McCarty, *Environmental Biotechnology: Principles and Applications*, McGraw-Hill Education, Columbus, OH, 2018.

40 A. Gjaltema, L. Tijhuis, M. C. van Loosdrecht and J. J. Heijnen, *Biotechnol. Bioeng.*, 1995, **46**, 258–269.

41 H. T. Chang, B. E. Rittmann, D. Amar, R. Heim, O. Ehlinger and Y. Lesty, *Biotechnol. Bioeng.*, 1991, **38**, 499–506.

42 C. Nicolella, R. Di Felice and M. Rovatti, *Biotechnol. Bioeng.*, 1996, **51**, 713–719.

43 A. Gjaltema, J. L. Vinke, M. C. van Loosdrecht and J. J. Heijnen, *Biotechnol. Bioeng.*, 1997, **53**, 88–99.

44 C. Shin, S. H. Tilmans, F. Chen and C. S. Criddle, *Chem. Eng. J.*, 2021, **426**, 131912.

45 A. Venu Vinod and G. Venkat Reddy, *J. Hazard. Mater.*, 2006, **136**, 727–734.

46 L. P. Lakshmi and Y. P. Setty, *Chem. Eng. J.*, 2008, **135**, 135–140.

47 C. Nicolella, M. C. van Loosdrecht, R. G. van der Lans and J. J. Heijnen, *Biotechnol. Bioeng.*, 1998, **60**, 627–635.

48 C. Nicolella, M. C. M. van Loosdrecht and J. J. Heijnen, *Chem. Eng. Sci.*, 1998, **53**, 2743–2753.
49 N. A. Shvab, *J. Appl. Electrochem.*, 2000, **30**, 1285–1292.
50 R. Zenit, M. L. Hunt and C. E. Brennen, *J. Fluid Mech.*, 1997, **353**, 261–283.
51 J. Jaafari, A. Mesdaghinia, R. Nabizadeh, M. Hoseini, H. Kamani and A. H. Mahvi, *J Environ Health Sci Eng*, 2014, **12**, 139.
52 C. Shin, E. Lee, P. L. McCarty and J. Bae, *Bioresour. Technol.*, 2011, **102**, 9860–9865.
53 C. Shin and J. Bae, *Bioresour. Technol.*, 2018, **247**, 1038–1046.
54 A. Gjaltema, M. C. van Loosdrecht and J. J. Heijnen, *Biotechnol. Bioeng.*, 1997, **55**, 206–215.